Chinese Journal of Chemical Engineering 88 (2025) 296–309

Contents lists available at ScienceDirect

Chinese Journal of Chemical Engineering

journal homepage: www.elsevier.com/locate/CJChE

Full Length Article

Globally optimal design of shell and tube heat exchangers under multi-scenario using set trimming

Kexin Zhu , Yi Cui , Yufei Wang *

College of Chemical Engineering and Environment, China University of Petroleum (Beijing), Beijing 102249, China

A R T I C L E I N F O

Article history:
Received 20 December 2024
Received in revised form
19 June 2025
Accepted 19 June 2025
Available online 13 August 2025

Keywords:
Double shell and tube heat exchangers
Set trimming
Optimisation

A B S T R A C T

With the energy problem becoming increasingly severe, industrial energy efficiency issues need to be solved urgently. The tube and shell heat exchanger, as the most widely used device for energy recovery and utilisation, its optimal design has become a significantly important research topic. Optimal design solves the tediousness of traditional design and can easily and accurately give the desired design results. Several industrial heat duty targets and pressure drop limitations for the design of shell-and-tube heat exchangers, such as high heat transfer efficiency, large temperature correction coefficient, and high capacity, cannot be met by single-shell units and require series or parallel arrangements. This paper uses Set Trimming to optimize the design of double shell and tube heat exchangers, assuming the possibility of series, parallel, or series-parallel arrangements. Minimum heat transfer area and minimum total annualized cost are used as objective functions to optimize the design of a single or double-shell heat exchanger that better meets the objectives.

1. Introduction

Economic development cannot be separated from industrial construction, and with the double-carbon goal, the problem of industrial energy saving needs to be solved [1–3]. Heat exchanger is a kind of heat transfer equipment, which is a key device for energy recovery and utilisation in factories [4]. The shell and tube heat exchanger is one of the most widely used heat exchangers in industrial production, which is very easy to fabricate and operate, and therefore it is used in petrochemical, power stations, ships, and other industries [5–8]. Traditional heat exchanger design requires guessing the heat exchanger parameters and then verifying them using a large number of 23 enumeration algorithms to determine the feasibility of the results [9–11]. This method requires experienced engineers to intervene and work for a long time, which is not only time-consuming and labour-intensive, but also often results in less than optimal results, so it is particularly important to optimize the design of heat exchangers and quickly seek optimal solutions.

There are many studies on the automatic design of heat exchangers, Han *et al.* [12] proposed an improved sparrow search algorithm for multi-objective optimal design of heat exchangers. Wang *et al.* [13] used a multi-objective optimisation method for numerical study of spiral coil heat exchangers. The heat transfer enhancement and flow characteristics were analysed by using sensitivity analysis. Goncalves *et al.* [14] used mixed integer linear programming method for optimal design of heat exchangers and achieved the global optimum. Foruzan Nia *et al.* [15] used a simulated annealing algorithm for the bi-objective optimal design of the heat exchanger. It has also been found that lower pressure drops can be achieved by placing the heat exchanger tube near the insulating wall. Khoshbadollahi *et al.* [16] used particle swarm algorithm for optimal design of plate-fin heat exchanger for waste heat recovery and proved that the return method affects the total annual cost and heat transfer efficiency. Pawar *et al.* [17] conducted experiments on the heat transfer characteristics of spiral coil heat exchangers using CFD simulations to find out the relevance of the Nussle number friction factor.

All these studies were conducted with a single-shell heat exchanger as an object for a small flow strand, aiming to prove the feasibility of automatic design. In industrial production, heat exchangers not only need to meet the design requirements in a single scenario, but also need to consider their applications in multiple scenarios. For the scenarios with high heat transfer efficiency and large processing capacity, a more suitable heat exchanger needs to be selected to meet the heat transfer requirements. Single-shell

* Corresponding author.
E-mail address: wangyufei@cup.edu.cn (Y. Wang).

https://doi.org/10.1016/j.cjche.2025.06.024
1004-9541/

heat exchanger due to its shell being less, needs to increase the number of tubes to improve heat transfer efficiency, and increasing the number of tubes will lead to the heat exchanger temperature correction coefficient being smaller, the heat exchanger can not work properly. In addition, the heat exchanger for heat transfer can handle the flow is limited, and in the face of the large processing capacity of a single heat exchanger used independently is difficult to meet the production requirements.

In the face of the small *Ft* value of the single-shell heat exchanger with multiple pipe strokes, present studies have been suggested that it can use the double-shell heat exchanger with *Ft* close to 1, which can realise the heat exchange of the cold and hot flow media under countercurrent conditions, which not only solves the problem of small *Ft* value of the single-shell heat exchanger, but also improves the heat exchange efficiency. At present, most of the research on the design of double-shell heat exchanger is to optimize its structure, such as joining the folding plate on the shell side [18,19], designing the shell as a multi-layer spiral coil structure [20], using continuous spiral baffle [21–24], adding casing on the heat exchanger [21], designing a closed double-shell structure [25], through which the heat exchange efficiency and energy utilisation can be improved in a higher degree. Heat transfer efficiency and improve energy utilisation.

In the face of high capacity, a single heat exchanger cannot work properly and needs to be designed in series or parallel with the aim of spreading the temperature or flow rate to achieve the heat transfer demand. Currently, the design of heat exchangers in series or parallel is based on a given series-parallel arrangement, and simulations [26,27] or experiments [28,29] are conducted to verify that a certain arrangement has a better heat transfer efficiency or overall performance.

However, in the above studies for double-shell heat exchanger, apart from structural optimisation, there is little research on the optimal design of the double-shell heat exchanger itself. Besides, the above research can give a better solution in series and parallel under certain conditions, they are all artificially set series and parallel, and the automatic series and parallel design of heat exchangers has not been addressed.

To better solve the above problems, the following contributions are made in this paper: in this paper, Set Trimming is applied to the design of a double-shell heat exchanger. Set Trimming was originally proposed by Gut and Pinto [30] for the specific case of plate heat exchanger design. Costa and Bagajewicz [31] refined its concept by extending it to any optimisation problem with discrete independent variables. Lemos *et al.* [28] developed the algorithm, used inequality constraint order to eliminate the infeasibility to obtain the heat exchanger design variables, with the objective of minimizing the heat exchange area, which significantly improved the computational efficiency. The algorithm uses a set of inequality constraints to generate a smaller subset by sequentially pruning it step by step until an optimal solution is found, which is not only fast and convenient, but also ensures the global optimality since it only eliminates infeasible options in the process, and finally, it is to select the best solution among all feasible candidates. Fig. 1 shows the procedure of Set Trimming. For the heat exchanger, the ratio range of shell diameter to tube length and the ratio range of shell diameter to plate spacing are first trimmed, and heat exchangers that do not satisfy the ratio range are eliminated. Then, the flow rate, Reynolds number, and pressure drop of the tube and shell processes are trimmed in that order. Finally, the heat transfer area is trimmed to select the heat exchanger that best meets the objective function.

In addition, this paper also proposes a new method of automatic design of heat exchanger series-parallel arrangement by the program. With the given parameters of the heat exchanger logistics, the flow rate, and temperature, the program automatically

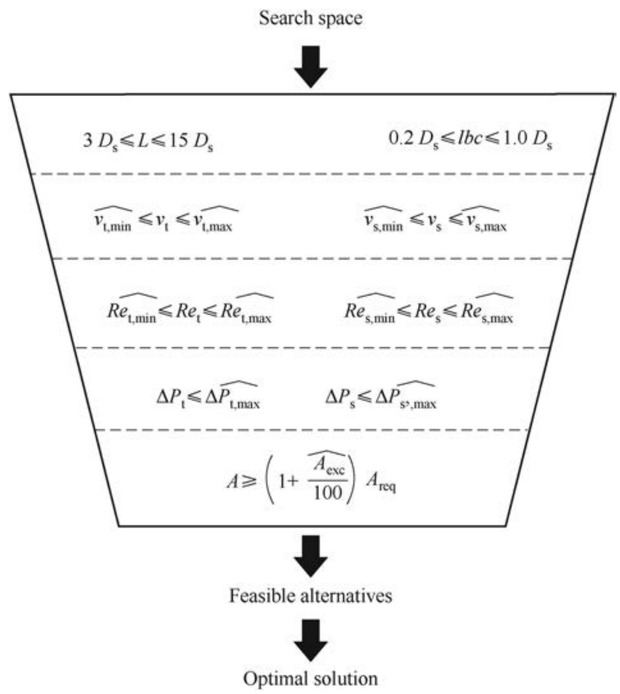

Fig. 1. The procedure of set trimming.

determines whether it is necessary to carry out the series-parallel connection and the case of series-parallel connection. Finally, give the heat exchanger arrangement, heat exchanger number, and the optimisation results. To a certain extent, this method not only reduces the design time but also eliminates the tedium caused by manual design. In addition, this method gives the optimal heat exchanger arrangement with a high degree of accuracy. The process of automatic series-parallel design is shown in the following. The process of automatic series-parallel design is shown in Fig. 2. Firstly, the program inputs the given logistic parameters, design parameters, and inlet and outlet temperatures. Then the heat exchanger design is carried out according to the input parameters, and the heat exchanger is screened in the face of the pressure drop constraints. If the pressure drop constraints can be met, the heat exchanger that best meets the objective function is obtained directly. If the pressure drop constraints cannot be met, then a split flow (series-parallel) design is required. The flow rate and inlet and outlet temperatures are reset, and the heat exchanger is designed based on the new parameters and compared to the pressure drop constraints. If the pressure drop constraints can be met, the parameters of the heat exchanger series-parallel and individual heat exchangers are obtained, and if the constraints still cannot be met, the above steps are repeated until the constraints are met to obtain the optimal heat exchanger arrangement and heat exchanger design.

What's more, this paper also establishes a complete set of mathematical models of the double-shell heat exchanger, which can better optimize the design of the double-shell heat exchanger.

2. Heat Exchanger Model and Inequality Constraints

Without loss of generality, the shell of heat exchanger has the following assumptions in this paper. This paper uses a fixed-tube-sheet heat exchanger without phase change. The physical parameters of the hot and cold streams are considered to be constant during the heat transfer process, and these parameters are represented with the symbol "ˆ".

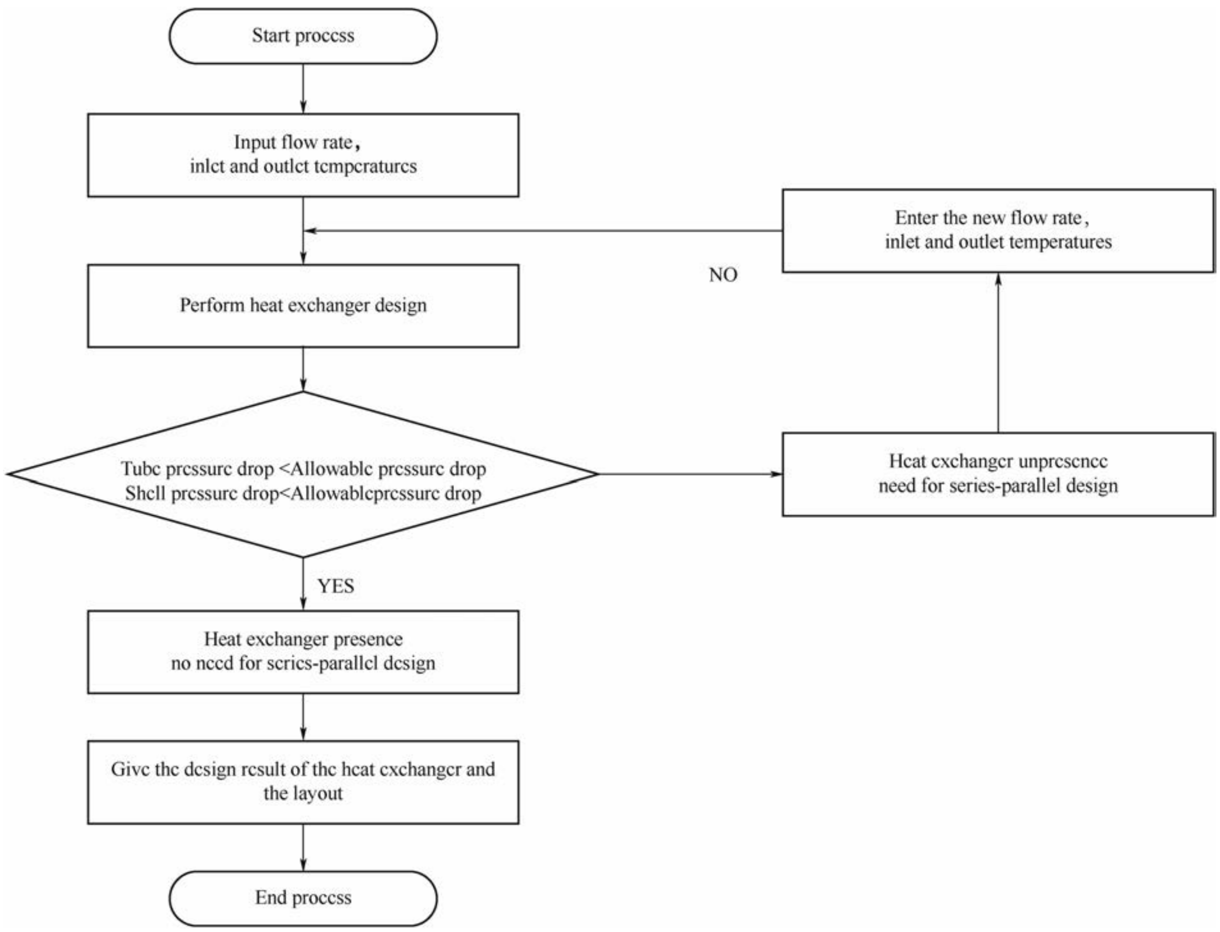

Fig. 2. Flow chart for automatic series-parallel design.

In this paper, based on the single-shell heat exchanger model proposed in the Ref. [14], the detailed calculation model, total heat transfer coefficient model, and heat duty model of the double-shell heat exchanger are extended. The two models have a high degree of consistency in theoretical basis and calculation logic. The single-shell heat exchanger model used in the paper is consistent with the model in the Ref. [14], and the double-shell heat exchanger model is as follows. This model has been validated in Aspen EDR with accuracy. The structure of single-shell heat exchanger and double-shell heat exchanger is shown in Fig. 3.

2.1. Double-shell heat exchanger model

2.1.1. Calculation methods

The optimal design of the heat exchanger is calculated for each parameter of fluid dynamics and thermodynamics in the following order.

The baffle spacing is calculated as:

$$l_{\mathrm{bc}}=\frac{L}{\frac{N_{\mathrm{b}}}{2}+1} \tag{1}$$

where L is the tube length and N_{b} is the number of baffles.

The free area ratio is calculated as:

$$\mathrm{FAR}=1-\frac{1}{r_{\mathrm{p}}} \tag{2}$$

where r_{p} is the ratio between the outer diameter of the tube and the pitch of the tube.

The shell flow area is calculated as:

$$A_r=\frac{D_{\mathrm{s}}}{2}\ \mathrm{FAR}\cdot\ l_{\mathrm{bc}} \tag{3}$$

where D_{s} is the shell diameter, FAR is the free area ratio and l_{bc} is the baffle spacing.

The shell flow velocity is calculated as:

$$v_{\mathrm{s}}=\frac{\widehat{m_{\mathrm{s}}}}{\widehat{\rho_{\mathrm{s}}}\ Ar} \tag{4}$$

where $\widehat{m_{\mathrm{s}}}$ is the shell mass flow rate, $\widehat{\rho_{\mathrm{s}}}$ is the shell fluid density, and Ar is the shell flow area.

The tube pitch is calculated as:

$$l_{\mathrm{tp}}=r_{\mathrm{p}}\ d_{\mathrm{te}} \tag{5}$$

where d_{te} is the outer tube diameter.

The total number of tubes is calculated as:

$$N_{\mathrm{tt}}=\mathrm{round}\left(\frac{\pi\ D_{\mathrm{s}}{}^2}{4\ l_{\mathrm{tp}}{}^2\ l_{\mathrm{ay}}\ F_{\mathrm{TC}}\ \widehat{F_{\mathrm{SC}}}}\right) \tag{6}$$

where D_{s} is the shell diameter, l_{tp} is the tube pitch, l_{ay} is the tube bundle layout parameter, take 0.866 when it is a triangular layout, and take 1 when it is a square layout. F_{TC} is the tube bundle correction coefficient, which is related to the selection of the number of tubes and the shell diameter, and the value is

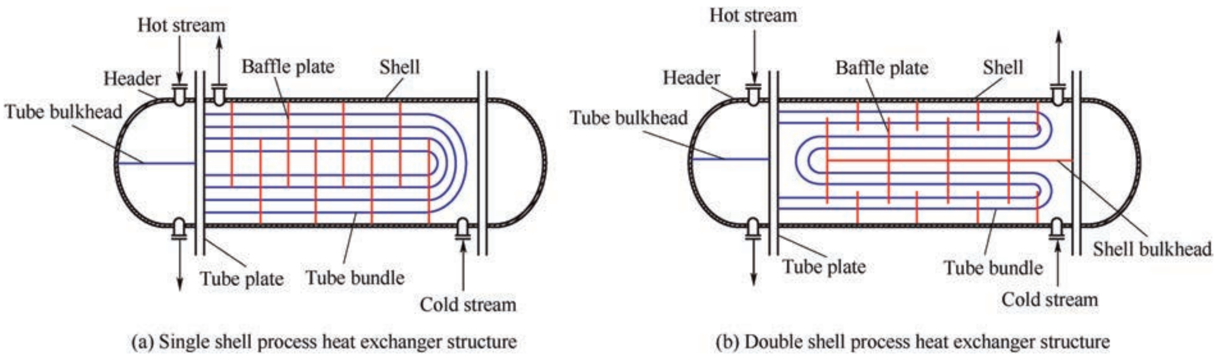

Fig. 3. Heat exchanger structural diagram.

shown in Table 1. $\widehat{F_{SC}}$ is the heat exchanger structure coefficient, which is related to the heat exchanger header type, and in this paper, we choose the fixed tube and plate header type, and the value of $\widehat{F_{SC}}$ is 1.0.

The number of tubes passing through each stream is calculated as:

$$N_{tp} = \frac{N_{tt}}{\widehat{N_{pt}}} \tag{7}$$

where N_{tt} is the total number of tubes and $\widehat{N_{pt}}$ is the number of tube passes.

The pipe flow rate is calculated as:

$$v_t = \frac{4\,\widehat{m_t}}{N_{tp}\,\pi\,\widehat{\rho_t}\,{d_{ti}}^2} \tag{8}$$

where $\widehat{m_t}$ is the tube mass flow rate, $\widehat{\rho_t}$ is the tube fluid density, and d_{ti} is the inlet tube diameter.

The equivalent diameter is calculated as:

$$D_{eq} = \frac{4\,{l_{tp}}^2}{\pi\,d_{te}} - d_{te}\ (\text{Square Layout}) \tag{9}$$

$$D_{eq} = \frac{3.46\,{l_{tp}}^2}{\pi\,d_{te}} - d_{te}\ (\text{Triangular Layout}) \tag{10}$$

The shell Reynolds number is calculated as:

$$Re_s = \frac{D_{eq}\,v_s\,\widehat{\rho_s}}{\widehat{\mu_s}} \tag{11}$$

where D_{eq} is the equivalent diameter, v_s is the shell flow rate, and $\widehat{\mu_s}$ is the shell fluid viscosity.

The tube Reynolds number is calculated as:

$$Re_t = \frac{d_{ti}\,v_t\,\widehat{\rho_t}}{\widehat{\mu_t}} \tag{12}$$

where v_s is the tube flow velocity and $\widehat{\mu_t}$ is the tube fluid viscosity.

The tube friction coefficient is calculated as:

$$f_t = 0.014 + \frac{1.056}{Re_t^{0.42}} \tag{13}$$

where Re_t is the tube Reynolds number.

The allowable pressure drop across the tube is calculated as:

$$\frac{\Delta P_t}{\widehat{\rho_t}\,\widehat{g}} = \frac{f_t\,\widehat{N_{pt}}\,L\,{v_t}^2}{2\,\widehat{g}\,d_{ti}} + \frac{\widehat{K}\,\widehat{N_{pt}}\,{v_t}^2}{2\,\widehat{g}} \tag{14}$$

where f_t is the tube friction coefficient, $\widehat{g}$ is the gravitational acceleration, and $\widehat{K}$ is the pressure drop parameter, which is taken as 1.6.

The shell friction coefficient is calculated as:

$$f_s = 1.728\,{Re_s}^{-0.188} \tag{15}$$

where Re_s is the shell Reynolds number.

The allowable pressure drop across the shell is calculated as:

$$\frac{\Delta P_s}{\widehat{\rho_s}\,\widehat{g}} = f_s \frac{D_s(N_b+1)}{D_{eq}} \left(\frac{{v_s}^2}{2\,\widehat{g}}\right) \tag{16}$$

where f_s is the shell friction coefficient.

The shell Prandtl number is calculated as:

$$\widehat{Pr_s} = \frac{\widehat{C_{ps}}\,\widehat{\mu_s}}{\widehat{k_s}} \tag{17}$$

where $\widehat{C_{ps}}$ is the shell fluid heat capacity and $\widehat{k_s}$ is the shell thermal conductivity.

The shell Nussle number is calculated as:

$$Nu_s = 0.36\,Re_s^{0.55}\,\widehat{Pr_s}^{\frac{1}{3}} \tag{18}$$

where $\widehat{Pr_s}$ is the shell Prandtl number.

The shell heat transfer coefficient is calculated as:

$$h_s = \frac{Nu_s\,\widehat{k_s}}{D_{eq}} \tag{19}$$

where Nu_s is the shell Nussel number.

Table 1
Values of tube bundle correction coefficient.

N_{tp}	F_{TC}
1	1.08
2	1.11
4, 6	$D_s \leq 0.635$m, 1.45
	$D_s > 0.635$m, 1.18

The tube Prandtl number is calculated as:

$$\widehat{Pr_t} = \frac{\widehat{C_{pt}}\ \widehat{\mu_t}}{\widehat{k_t}} \tag{20}$$

where $\widehat{C_{pt}}$ is the tube fluid heat capacity and $\widehat{k_t}$ is the tube thermal conductivity.

The tube Nussell number is calculated as:

$$Nu_t = 0.023\ Re_t^{0.8} \widehat{Pr_t}^{n} \tag{21}$$

where $\widehat{Pr_t}$ is the tube Prandtl number, n is 0.3 when the fluid is cooled and 0.4 when the fluid is heated.

The tube heat transfer coefficient is calculated as:

$$h_t = \frac{Nu_t\ \widehat{k_t}}{d_{ti}} \tag{22}$$

where Nu_t is the tube Nussell number.

2.1.2. Calculation of total heat transfer coefficient

The total heat transfer coefficient is calculated as:

$$U = \frac{1}{\frac{d_{te}}{d_{ti}\ h_t} + \frac{\widehat{R_{ft}}\ d_{te}}{d_{ti}} + \frac{d_{te}\ \ln\left(\frac{d_{te}}{d_{ti}}\right)}{2\ \widehat{k_{tube}}} + \widehat{R_{fs}} + \frac{1}{h_s}} \tag{23}$$

where h_t, h_s are tube and shell heat transfer coefficients, $\widehat{R_{ft}}$ is the tube fouling coefficient, $\widehat{k_{tube}}$ is the tube variable heat transfer coefficient, and $\widehat{R_{fs}}$ is the shell fouling coefficient.

2.1.3. Calculation of heat duty

The heat duty is calculated as:

$$\widehat{Q} = \widehat{C_{pt}}\ \widehat{m_t}\ \widehat{\Delta T_t} \tag{24}$$

where $\widehat{\Delta T_t}$ is the temperature difference between the inlet and outlet of the tube flow stream.

The logarithmic mean temperature difference is calculated as:

$$\widehat{\Delta T_{lm}} = \frac{\left(\widehat{T_{h,i}} - \widehat{T_{c,o}}\right) - \left(\widehat{T_{h,o}} - \widehat{T_{c,i}}\right)}{\ln\left(\frac{\left(\widehat{T_{h,i}} - \widehat{T_{c,o}}\right)}{\widehat{T_{h,o}} - \widehat{T_{c,i}}}\right)} \tag{25}$$

where $\widehat{T_{h,o}}$ is the hot outlet temperature, $\widehat{T_{h,i}}$ is the hot inlet temperature, $\widehat{T_{c,o}}$ is the cold outlet temperature, and $\widehat{T_{c,i}}$ is the cold inlet temperature.

The correction coefficient for LMTD is calculated [29] as:

$$\widehat{F} = \frac{\frac{\sqrt{\widehat{R}^2+1}}{\widehat{R}-1}\ \ln\left(\frac{1-\widehat{P}\ \widehat{R}}{1-\widehat{P}}\right)^{\frac{1}{N}}}{\ln\left[\frac{1+\left(\frac{1-\widehat{P}\ \widehat{R}}{1-\widehat{P}}\right)^{\frac{1}{N}} - \frac{\sqrt{\widehat{R}^2+1}}{\widehat{R}-1} + \frac{\sqrt{\widehat{R}^2+1}}{\widehat{R}-1}\left(\frac{1-\widehat{P}\ \widehat{R}}{1-\widehat{P}}\right)^{\frac{1}{N}}}{1+\left(\frac{1-\widehat{P}\ \widehat{R}}{1-\widehat{P}}\right)^{\frac{1}{N}} + \frac{\sqrt{\widehat{R}^2+1}}{\widehat{R}-1} - \frac{\sqrt{\widehat{R}^2+1}}{\widehat{R}-1}\left(\frac{1-\widehat{P}\ \widehat{R}}{1-\widehat{P}}\right)^{\frac{1}{N}}}\right]}\ (\widehat{R} \neq 1) \tag{26}$$

$$\widehat{F} = \sqrt{2}\ \frac{\widehat{P}}{\widehat{N} - \widehat{N}\widehat{P}}\ \frac{1}{\ln\left[\frac{\frac{(\widehat{N}-\widehat{N}\ \widehat{P})}{\widehat{P}} + \frac{1}{\sqrt{2}}}{\frac{(\widehat{N}-\widehat{N}\ \widehat{P})}{\widehat{P}} - \frac{1}{\sqrt{2}}}\right]}\ (\widehat{R} = 1) \tag{27}$$

where $\widehat{N}$ is the shell number and is taken as 2 in this paper.

The correlation coefficient in LMTD is calculated as:

$$\widehat{R} = \frac{\widehat{T_{h,i}} - \widehat{T_{h,o}}}{\widehat{T_{c,o}} - \widehat{T_{c,i}}} \tag{28}$$

$$\widehat{P} = \frac{\widehat{T_{c,o}} - \widehat{T_{c,i}}}{\widehat{T_{h,i}} - \widehat{T_{c,i}}} \tag{29}$$

2.1.4. Calculation of heat transfer area

The required area is calculated as:

$$A_{req} = \frac{\widehat{Q}}{U\ \widehat{\Delta T_{lm}}\ \widehat{F}} \tag{30}$$

where $\widehat{Q}$ is the heat duty, U is the total heat transfer coefficient, $\widehat{\Delta T_{lm}}$ is the logarithmic mean temperature difference, and $\widehat{F}$ is the correction coefficient.

The heat transfer area is calculated as:

$$A = N_{tt}\ \pi\ d_{te}\ L \tag{31}$$

2.2. Constraints [28]

The constraints on the tube length and shell diameter are calculated as:

$$L \geq 3\ D_s \tag{32}$$

$$L \leq 15\ D_s \tag{33}$$

The constraints on the baffle spacing are calculated as:

$$l_{bc} \geq 0.2\ D_s \tag{34}$$

$$l_{bc} \leq 1.0\ D_s \tag{35}$$

The constraints on the flow velocity are calculated as:

$$v_s \geq \widehat{v_{s,min}} \tag{36}$$

$$v_s \leq \widehat{v_{s,max}} \tag{37}$$

$$v_t \geq \widehat{v_{t,min}} \tag{38}$$

$$v_t \leq \widehat{v_{t,max}} \tag{39}$$

The constraint on the Reynolds number is calculated as:

$$Re_s \geq 2 \times 10^3 \tag{40}$$

$$Re_t \geq 10^4 \tag{41}$$

In the process design, the allowable pressure drop is imposed

Table 2
Design data.

Example	1		2		3		4	
Service	Crude oil cooler		Crude oil cooler		Methanol heater		Sucrose solution heater	
Stream allocation	Tube	Shell	Tube	Shell	Tube	Shell	Tube	Shell
Fluid	Cooling water	Crude oil	Cooling water	Crude oil	Hot water	Methanol	Hot water	Sucrose
Tube fluid	Cold		Cold		Hot		Hot	
Mass flow rate, $\widehat{m}$/kg·s^{-1}	228.8	110	130.0	50.0	40	133.3	40	133.3
Inlet temperature, $\widehat{T}$/°C	30	90	30	100	220	30	220	30
Outlet temperature, $\widehat{T}$/°C	40	50	40	50	110.2	80	80.8	80
Density, $\widehat{\rho}$/kg·m^{-3}	995	786	995	786	888	750	888	1080
Viscosity, $\widehat{\mu}$/mPa·s	0.72	1.89	0.72	1.89	0.15	0.34	0.15	1.30
Heat capacity, $\widehat{c_p}$/J·kg^{-1}·K^{-1}	4187	2177	4187	2177	4312	2840	4312	3601
Thermal conductivity, $\widehat{k}$/W·m^{-1}·K^{-1}	0.59	0.12	0.59	0.12	0.7	0.19	0.70	0.58
Fouling factor, $\widehat{R_f}$/m^2·K·W^{-1}	0.0004	0.0002	0.0003	0.0002	0.0001	0.0001	0.0001	0.0001
Allowable pressure drop, Δ*P*/kPa	100	100	50	100	70	70	100	100
Flow velocity bounds/m·s^{-1}	[0.5,2]	[0.5,2]	[0.5,2]	[0.5,2]	[0.5,2]	[1,3]	[0.5,2]	[1,3]

based on the pressure distribution of the device. The relevant constraints are calculated as:

$$\Delta P_s \le \Delta\widehat{P_{s,\max}} \tag{42}$$

$$\Delta P_t \le \Delta\widehat{P_{t,\max}} \tag{43}$$

The constraint between heat transfer area and excess area is calculated as:

$$A \ge \left(1 + \frac{\widehat{A_{exc}}}{100}\right)\cdot A_{req} \tag{44}$$

2.3. Objective function

The two main objective functions optimized in this paper are:

(1) Min A (minimum heat transfer area); (2) Min TAC (minimum total annualized cost).

In this case, the heat transfer area is calculated as Eq. (31), and the total annual cost [32] is calculated as Eq. (45):

$$\mathrm{TAC} = \widehat{af}\left(\widehat{\alpha}A^{0.8}\right) + \widehat{\mathrm{EC}}\widehat{\mathrm{Hour}}\left(\frac{\widehat{m_s}\,\Delta P_s}{\widehat{\rho_s}\,\widehat{\eta}} + \frac{\widehat{m_t}\,\Delta P_t}{\widehat{\rho_t}\,\widehat{\eta}}\right) \tag{45}$$

where $\widehat{af}$ is the annual interest rate, which is calculated as shown in Eq. (46). $\widehat{\alpha}$ is the cost parameter of the heat exchanger, which is taken as 20 [33]; $\widehat{\mathrm{EC}}$ is the electricity costs, which is taken as 0.12 USD·kW·h^{-1}; $\widehat{\mathrm{Hour}}$ is the annual running time, which is taken as 8000 h·a^{-1}; and $\widehat{\eta}$ is the motor efficiency, which is taken as 75%.

$$\widehat{af} = \frac{\widehat{i}(1+\widehat{i})^{\widehat{n_y}}}{(1+\widehat{i})^{\widehat{n_y}} - 1} \tag{46}$$

where $\widehat{i}$ is the rate of deprecation, taken as 10%, and $\widehat{n_y}$ is the cost recovery period, taken as 5 years.

3. Single-shell and Double-shell Heat Exchanger Case Study

In this paper, an excess area $\widehat{A_{exc}}$ of 11%, a tube wall thickness of 1.65 mm and a wall thermal conductivity $\widehat{k_{tube}}$ of 50 W·m^{-1}·K^{-1} are considered for optimisation. The programmes of the research are run in GAMS 24.2.3 and MATLAB R2023a.

Table 2 shows the flow parameters for cold and hot streams, inlet and outlet temperatures, the maximum permissible pressure drop and the range of flow rates. Table 3 shows the standard values of the discrete design variable and the data is taken from the Ref. [14]. The double-shell heat exchanger designed in this research is a double-shell and four-tube heat exchanger.

3.1. Min A

To find out the design with smaller area in each group of cases, the single-shell heat exchanger and double-shell heat exchanger were optimized with the design objective of minimizing the heat transfer area. The design solutions are shown in Table 4 and the optimisation results are shown in Table 5 and Fig. 4. The complete design solutions and optimisation results are shown in the Appendix.

According to the design, it is found that under the same conditions, the temperature difference correction coefficient of single-shell heat exchanger is smaller than that of double-shell heat

Table 3
Standard values of the discrete design variables.

Variable	Values
Outer tube diameter, d_{te}/m	0.019, 0.025, 0.032, 0.038, 0.051
Tube length, *L*/m	1.220, 1.829, 2.439, 3.049, 3.659, 4.877, 6.098
Number of tube passes, N_{pt}	1, 2, 4, 6
Tube pitch ratio, t_p	1.25, 1.33, 1.50
Tube layout, l_{ay}	1 = Square, 2 = Triangular
Number of baffles, N_b	1, 2, 3, …, 20
Shell diameter, D_s/m	0.787, 0.838, 0.889, 0.940, 0.991, 1.067, 1.143, 1.219, 1.372, 1.524

Table 4
Design solutions for Min A.

Example	1	2	3	4
Heat exchanger type	Single	Single	Double	Double
Outer tube diameter, d_{te}/m	0.019	0.019	0.032	0.019
Tube length, L/m	6.098	6.098	3.049	4.877
Tube pitch ratio, r_p	1.25	1.25	1.33	1.50
Tube layout, l_{ay}	Square	Triangular	Square	Triangular
Shell diameter, D_s/m	1.219	0.787	0.787	0.838
Number of baffles , N_b	10	10	6	10
Number of tube passes, N_{pt}	2	4	4	4

Table 5
Optimisation results for Min A.

Example	1	2	3	4
Area/m^2	678.5	326.5	69.9	193.3
Temperature correction coefficient, F	0.931	0.929	0.980	0.961
Total number of tubes, N_{tt}	1864	897	228	664
Baffle spacing, l_{bc}/m	0.55	0.55	0.76	0.82
Tube pitch, l_{tp}/m	0.024	0.024	0.043	0.029
Shell-side flow velocity, v_s/m·s^{-1}	1.04	0.73	2.39	1.09
Tube-side flow velocity, v_t/m·s^{-1}	1.27	1.51	1.22	1.40
Shell-side heat transfer coefficient, h_s/W·m^{-2}·K^{-1}	1053.39	1001.53	2489.05	3943.95
Tube-side heat transfer coefficient, h_t/W·m^{-2}·K^{-1}	5934.83	6778.30	9825.24	12374.4
Overall heat transfer coefficient, U/W·m^{-2}·K^{-1}	533.75	562.96	1313.08	1643.07
Shell-side pressure drop, ΔP_s/Pa	95659	47638	50692	53798
Tube-side pressure drop, ΔP_t/Pa	20409	27602	9920	28894

exchanger. However, when the temperature difference between the inlet temperatures of the two streams is small (example 1 and example 2), the difference between the temperature difference correction coefficient of the two heat exchangers is not significant, and the tube diameter of the single-shell heat exchanger is designed to be smaller, so its heat transfer area is smaller. The heat transfer efficiency is also better. When the temperature difference between the inlet temperatures of the two streams is large (example 3 and example 4), the temperature difference correction coefficient of the double-shell heat exchanger is almost close to 1, and the number of tubes of the heat exchanger is designed to be smaller, so its heat transfer area is smaller. It can be concluded that when the temperature difference is small, the single-shell heat exchanger can meet the heat transfer needs, and the heat transfer area required is also smaller; when the temperature difference is large, the single-shell process heat exchanger can not meet the demand for heat transfer, it is necessary to use the double-shell process heat exchanger to achieve better heat transfer capacity.

In this paper, the design results of this research are compared with the literature [14], and the comparison results are shown in Table 6 and Fig. 5.

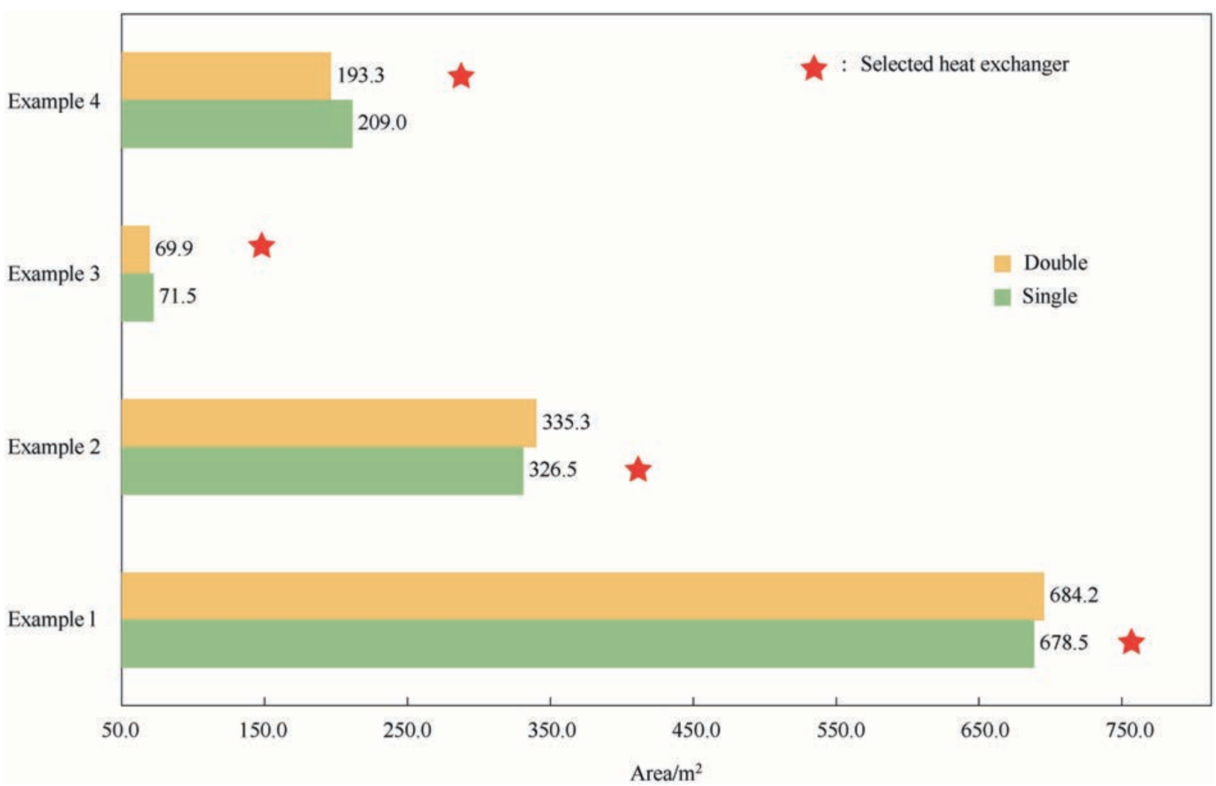

Fig. 4. Comparison chart of area optimisation results.

Table 6
Comparison of flow rate and area results from literature and research.

	Example 1	Example 2	Example 3	Example 4
Literature shell flow velocity bounds/m·s^{-1}	[1,3]	[1,3]	[1,3]	[1,3]
Literature area/m^2	624	319	144	207
Research shell flow velocity bounds/m·s^{-1}	[0.5,2]	[0.5,2]	[1,3]	[1,3]
Research area/m^2	678.5	326.5	69.9	193.3

Comparing this research with the literature, it is found that the optimisation results are better than the literature results when the design results are for double-shell heat exchanger. However, the optimisation results of the research are not as good as the literature when the design results are single-shell heat exchanger. This is because in the optimisation of this research, the shell fluid in example 1 and example 2 is crude oil, based on their properties such as viscosity and to ensure the operational safety of the double-shell heat exchanger, this research reduces the range of flow rates and hence the results from the literature are better. In examples 3 and 4, the viscosity of the shell fluid is lower, and it enables the safe operation of the double-shell heat exchanger, so there is no need to reduce the flow rate range. Under the same conditions, it can be seen that the methodology of this research can optimize the design of the heat exchanger reasonably effectively and obtain the optimal solution.

For this design, the purpose is to use the double-shell heat exchanger with better heat transfer efficiency to replace the single-shell heat exchanger, and from examples 1 and 2, it can be clearly seen that the single-shell heat exchanger heat transfer efficiency is better. This is mainly due to the fact that the allowable pressure drop is too small. As the number of shell increases, the pressure drop of the double-shell heat exchanger also needs to be larger. Therefore, taking example 1 as an example, the allowable pressure drop is modified. A sensitivity analysis of the relationship between the allowable pressure drop and the heat transfer area was done, and it can be seen from Fig. 6 that the design of the heat exchanger no longer changes when the allowable pressure drop ranges from 170 kPa onwards, so the allowable pressure drop was changed from 100 kPa to 200 kPa for a better comparison of single-shell heat exchanger and double-shell heat exchanger. The results obtained are shown in Table 7.

According to Table 7, it can be seen that when the constraints are relaxed, the optimized double-shell heat exchanger has a smaller heat transfer area, a larger temperature correction coefficient, and its total heat transfer coefficient is increased by 10.19%. Therefore, it is concluded that the use of double-shell heat exchanger can effectively solve the problem of low heat transfer efficiency of single-shell heat exchanger.

3.2. Min TAC

To find out the design with lower TAC in each group of cases, the single-shell heat exchanger and double-shell heat exchanger were optimized with the design objective of minimizing TAC. The design solutions are shown in Table 8 and the optimisation results are shown in Table 9 and Fig. 7. The

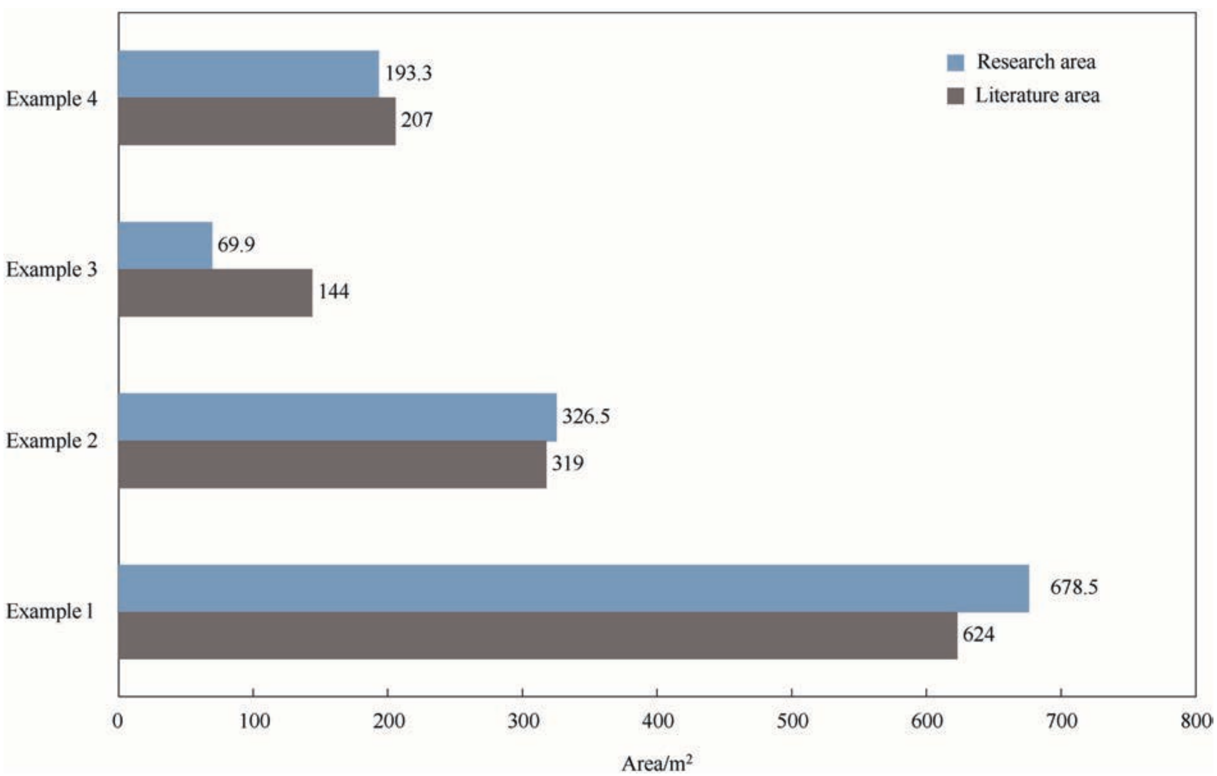

Fig. 5. Area comparison of literature and research.

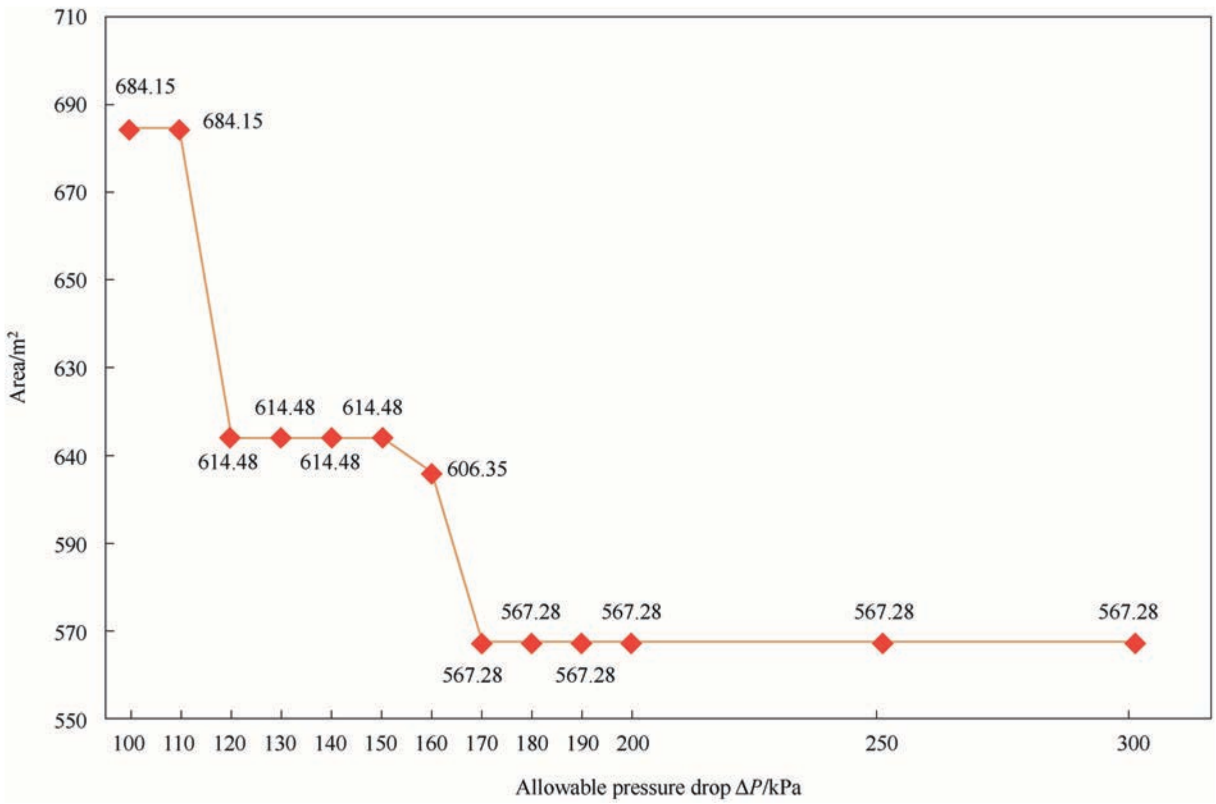

Fig. 6. Sensitivity analysis diagram.

Table 7
Optimisation results for Min A after correcting the pressure drop.

Optimisation results	Example 1	
	Single	Double
Area/m^2	678.5	567.3
Temperature correction coefficient, F	0.931	0.984
Shell-side heat transfer coefficient, h_s/W·m^{-2}·K^{-1}	1053.39	1193.32
Tube-side heat transfer coefficient, h_t/W·m^{-2}·K^{-1}	5934.83	6936.44
Overall heat transfer coefficient, U/W·m^{-2}·K^{-1}	533.75	588.13

Table 8
Design solutions for Min TAC.

Example	1	2	3	4
Heat exchanger type	Single	Double	Double	Double
Outer tube diameter, d_{te}/m	0.019	0.032	0.038	0.025
Tube length, L/m	6.098	6.098	3.659	4.877
Tube pitch ratio, r_p	1.25	1.25	1.50	1.33
Tube layout, l_{ay}	Triangular	Triangular	Square	Square
Shell diameter, D_s/m	1.219	1.067	1.143	0.991
Number of baffles, N_b	5	14	6	8
Number of tube passes, N_{pt}	1	4	4	4

complete design solutions and optimisation results are shown in the Appendix.

From example 1, it is known that the single-shell heat exchanger is better optimized when the inlet flow rate is higher. This is due to the higher number of tubes in the double-shell heat exchanger, the higher tube flow rate, its tube pressure drop increases substantially and the cost is higher. However, it can be seen from examples 2 to 4 that when the inlet flow rate is lower, the number of shells in the double-shell heat exchanger increases and the shell pressure drop is dispersed, resulting in a lower shell pressure drop and its TAC is lower. It can be seen that the TAC is not only related to the structure of the heat exchanger (number of shells), but also has a certain connection with its inlet flow rate. When double-shell heat exchanger is in the face of lower inlet flow, the flow distribution of the tube and shell is more even and can effectively reduce the cost of pressure drop; but in the face of higher inlet flow, the structure of the double-shell heat exchanger is more cumbersome, and its handling of the tube flow strand is not as good as a single-shell process, so the cost is higher.

Table 9
Optimisation results for Min TAC.

Example	1	2	3	4
Cost TAC/USD	6261	3343	2258	7407
Area/m^2	805.1	460.5	117.1	226.4
Total number of tubes, N_{tt}	2212	791	268	591
Baffle spacing, l_{bc}/m	1.02	0.81	0.92	0.98
Tube pitch, l_{tp}/m	0.024	0.047	0.057	0.033
Shell-side flow velocity, v_s/m·s	0.57	0.51	1.02	1.03
Tube-side flow velocity, v_t/m·s	0.54	0.70	0.71	0.82
Shell-side pressure drop, ΔP_s/Pa	25344	21457	8005	41426
Tube-side pressure drop, ΔP_t/Pa	2062	5278	3438	7949

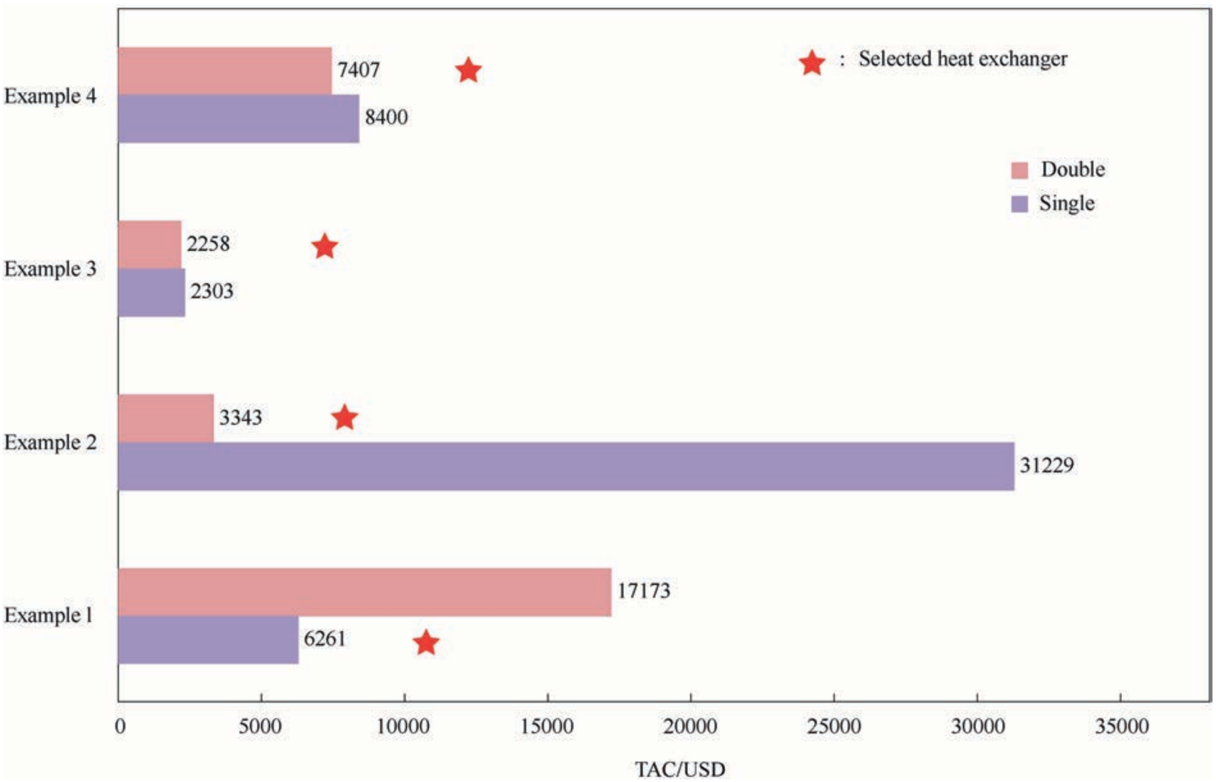

Fig. 7. Comparison chart of TAC optimisation results.

Table 10
Design data.

Service	Sucrose solution heater	
Stream allocation	Tube	Tube
Fluid	Hot water	Hot water
Tube fluid	Hot	
Mass flow rate, $\widehat{m}$/kg·s^{-1}	1500	4998.75
Inlet temperature, $\widehat{T}$/°C	220	30
Outlet temperature, $\widehat{T}$/°C	80.8	80
Density, $\widehat{\rho}$/kg·m^{-3}	888	1080
Viscosity, $\widehat{\mu}$/mPa·s	0.15	1.30
Heat capacity, $\widehat{c}_p$/J·kg^{-1}·K^{-1}	4312	3601
Thermal conductivity, $\widehat{k}$/W·m^{-1}·K^{-1}	0.70	0.58
Fouling factor, $\widehat{R}_f$/m^2·K·W^{-1}	0.0001	0.0001
Allowable pressure drop, ΔP/kPa	100	100
Flow velocity bounds/m·s^{-1}	[0.5,2]	[1,3]

4. Automatic Series-Parallel Design

Table 10 shows the flow parameters for cold and hot streams, inlet and outlet temperatures, the maximum permissible pressure drop and the range of flow rates. The design variables are kept consistent with Table 3. To minimise the TAC as the design objective of the single-shell heat exchanger and double-shell heat exchanger series-parallel automatic optimisation design, the optimisation results are shown in Table 11. The complete design solutions and optimisation results are shown in the Appendix.

According to the above table, it can be seen that when the inlet flow rate is very large, the heat exchanger can not meet the demand for heat transfer independently. After the series-parallel design, it can be seen that both single-shell heat exchanger and double-shell heat exchanger are designed to be arranged in parallel. Because of the large inlet flow and high heat load, when a series arrangement is used, the TAC is higher and economic efficiency is lower. What's more, the number of heat exchangers in series is larger, and when heat exchanges are performed, the temperature difference between the cold and hot flow strands of the intermediate heat exchangers is too small to satisfy the

Table 11
Optimisation results for automatic series-parallel connection.

Heat exchanger arrangement	Independent arrangement		Series-Parallel arrangement	
Heat exchanger type	Single	Double	Single	Double
Heat exchanger arrangement	–	–	Parallel	Parallel
Number of heat exchangers	–	–	8	16
Cost TAC/USD	–	–	601184	205040
Area/m^2	–	–	1081.8	492.8
Shell-side pressure drop, ΔP_s/Pa	–	–	97673	26538
Tube-side pressure drop, ΔP_t/Pa	–	–	5197	16544

demand for mutual heat exchange. The current industrial production is also the majority of the parallel arrangement. The method can quickly and accurately give the series-parallel scheme after the given flow rate and flow parameters, and can find out the lower TAC arrangement. From the above table, it can be seen that the TAC is reduced by 65.90% for parallel connection of double-shell heat exchanger at this flow rate. This is mainly due to the fact that with the increasing number of double-shell heat exchangers, the flow is spread out considerably, and the cost of each heat exchanger is reduced considerably. So, its total TAC is lower.

5. Conclusions

In this paper, Set Trimming has been used to optimize the design of single-shell heat exchanger and double-shell heat exchanger. With minimizing the heat exchange area and minimizing the TAC as the heat exchange objective can solve the problem of the small temperature difference correction coefficient and the high capacity. Facing these two conditions, the following conclusions can be drawn from the optimized design:

Under the premise of independent arrangement of heat exchangers, when the temperature difference between the inlet and outlet of the logistics is large, the use of double-shell heat exchanger can get a smaller heat exchange area. When the temperature difference between the inlet and outlet of the logistics is small, the use of single-shell heat exchanger can get a smaller heat exchange area. When the inlet flow rate is small, the use of double-shell heat exchanger TAC is smaller. When the inlet flow rate is large, the use of single-shell heat exchanger TAC is smaller.

In the face of high capacity and large inlet flow rate of logistics, this paper designs a new method for automatic series-parallel design. With the given logistics, this paper gives a design solution with optimisation results for the smallest TAC. It is found that the parallel arrangement of heat exchangers can solve the heat exchange problem better, and the cost of double-shell heat exchanger is reduced by 65.90% compared with single-shell heat exchanger.

CRediT Authorship Contribution Statement

Kexin Zhu: Writing – original draft, Methodology, Investigation. Yi Cui: Validation, Methodology. Yufei Wang: Writing – review & editing, Supervision, Conceptualization.

Declaration of Competing Interest

The authors declare that they have no known competing financial interests or personal relationships that could have appeared to influence the work reported in this paper.

Acknowledgements

Financial support from the National Natural Science Foundation of China under Grant (22393954) is gratefully acknowledged.

Nomenclature

A	heat transfer area, m^2
$\widehat{A_{exc}}$	excess area, %
A_r	shell flow area, m^2
A_{req}	required area, m^2
$\widehat{af}$	annual interest rate, %
$\widehat{C_p}$	heat capacity, $J\cdot(kg\cdot K)^{-1}$
D_{eq}	equivalent diameter, m
D_s	shell diameter, m
d_{te}	outer tube diameter, m
d_{ti}	inlet tube diameter, m
$\widehat{EC}$	electricity costs, $USD\cdot kW\cdot h^{-1}$
$\widehat{F}$	correction coefficient for LMTD method
FAR	free area ratio
$\widehat{F_{sc}}$	structure coefficient
F_{TC}	tube bundle correction coefficient
f	friction factor
$\widehat{g}$	gravitational acceleration, $g\cdot s^{-2}$
$\widehat{Hour}$	annual running time, $h\cdot a^{-1}$
h	heat transfer coefficient, $W\cdot(m^2\cdot K)^{-1}$
$\widehat{i}$	rate of deprecation, %
$\widehat{K}$	pressure drop parameters
k	thermal conductivity, $W\cdot(m\cdot K)^{-1}$
L	tube length, m
l_{ay}	layout
l_{bc}	baffle spacing, m
l_{tp}	tube pitch, m
m	mass flow rate, $kg\cdot s^{-1}$
$\widehat{N}$	shell number
N_b	number of baffles
$\widehat{N_{pt}}$	number of tube passes
N_{pt}	number of tubes per pass
N_{tt}	total number of tubes
Nu	Nusselt number
$\widehat{n}$	cost recovery period year
$\widehat{P}$	parameter used to calculate the correction coefficient
$\widehat{Pr}$	Prandtl number
ΔP	pressure drop, Pa
$\widehat{Q}$	heat duty, W
$\widehat{R}$	parameter used to calculate the correction coefficient
Re	Reynolds number
$\widehat{R_f}$	fouling factor, $m^2\cdot K\cdot W^{-1}$
r_p	tube pitch ratio
$\widehat{T}$	temperature, °C
TAC	total annualized cost, $USD\cdot a^{-1}$
$\widehat{\Delta T}$	inlet and outlet temperature difference, °C
$\widehat{\Delta T_{lm}}$	logarithmic mean temperature difference, °C
U	overall heat transfer coefficient, $W\cdot(m^2\cdot K)^{-1}$
v	flow velocity, $m\cdot s^{-1}$
$\widehat{\alpha}$	cost parameter
$\widehat{\eta}$	motor efficiency, %
$\widehat{\mu}$	viscosity, Pa·s
$\widehat{\rho}$	density, $kg\cdot m^{-3}$

Subscript

i	inlet
max	maximum value
min	minimum value
o	outlet
s	tube-side
t	shell-side
tube	heat exchanger tube variable
y	year

Superscript

n	heat and cold flow parameters

References

[1] W. Ye, W. Chaiyapa, Y.T. Li, A comparative study of energy governance on energy resilience: process tracing of China and Thailand's solar power development, *Energy Strategy Rev.* 55 (2024) 101500.
[2] B. Wang, K.Y. Dong, W.L. Zhong, C. Zhao, Can high-quality energy development and energy security achieve a win-win situation? The case of China, *Econ. Anal. Pol.* 83 (2024) 17–28.
[3] B.H. Jiang, M.Y. Raza, Research on China's renewable energy policies under the dual carbon goals: a political discourse analysis, *Energy Strategy Rev.* 48 (2023) 101118.
[4] N. Sohrabi, K.A. Hammoodi, A. Hammoud, D.J. Jasim, S.H. Hashemi Karouei, J. Kheyri, H. Nabi, Using different geometries on the amount of heat transfer in a shell and tube heat exchanger using the finite volume method, *Case Stud. Therm. Eng.* 55 (2024) 104037.
[5] M. Alhuyi Nazari, M.H. Ahmadi, A. Mukhtar, V. Blazek, L. Prokop, S. Misak, Intelligent techniques for prediction characteristics of shell and tube heat exchangers: a comprehensive review, *Int. Commun. Heat Mass Tran.* 158 (2024) 107864.
[6] S. Saha, N. Hasan, Numerical evaluation of thermohydraulic parameters for diverse configurations of shell-and-tube heat exchanger, *Results Eng.* 23 (2024) 102509.
[7] C.L. Chang, W.F. Shen, Global optimization of the design of intensified shell and tube heat exchanger using tube inserts, *Can. J. Chem. Eng.* 102 (1) (2024) 350–365.
[8] S.P. He, M.J. Wang, W.X. Tian, S.Z. Qiu, G.H. Su, Development of an OpenFOAM solver for numerical simulations of shell-and-tube heat exchangers based on porous media model, *Appl. Therm. Eng.* 210 (2022) 118389.
[9] R.W. Serth, T.G. Lestina, Process Heat Transfer: Principles, Applications and Rules of Thumb, Elsevier/Academic Press, Amsterdam and Boston, 2014.
[10] K.J. Bell, Heat exchanger design for the process industries, *J. Heat Tran.: Transactions of the ASME* 126 (6) (2004) 877–885.
[11] E. Cao, Heat Transfer in Process Engineering, McGraw-Hill, New York,USA, 2010.
[12] S.S. Han, X.T. Li, Z.M. Liu, B.J. Zhang, C. He, Q.L. Chen, Thermal-economic optimization design of shell and tube heat exchanger using an improved sparrow search algorithm, *Therm. Sci. Eng. Prog.* 45 (2023) 102085.
[13] G.H. Wang, D.B. Wang, J. Deng, Y.M. Lyu, Y.S. Pei, S. Xiang, Experimental and numerical study on the heat transfer and flow characteristics in shell side of helically coiled tube heat exchanger based on multi-objective optimization, *Int. J. Heat Mass Tran.* 137 (2019) 349–364.
[14] C. Gonçalves, A.L.H. Costa, M.J. Bagajewicz, Shell and tube heat exchanger design using mixed-integer linear programming, *AIChE J.* 63 (6) (2017) 1907–1922.
[15] M. Foruzan Nia, H. Farzad, A. Babak Ansari, M. Ghodrat, S. Abdolreza Gandjalikhan Nassab, M. Behnia, Performance improvement of a tubular heat exchanger by tube arrangement optimization using simulated annealing algorithm and blocked-off method, *Therm. Sci. Eng. Prog.* 40 (2023) 101793.
[16] A. Khoshbakht, H. Hajabdollahi, M. Shafiey Dehaj, Investigating the effect of stream reflux on optimum design of heat exchanger using Particle Swarm Algorithm, *J. Taiwan Inst. Chem. Eng.* 144 (2023) 104745.
[17] S.S. Pawar, V.K. Sunnapwar, Experimental and CFD investigation of convective heat transfer in helically coiled tube heat exchanger, *Chem. Eng. Res. Des.* 92 (11) (2014) 2294–2312.
[18] X.T. Wang, N.B. Zheng, P. Liu, Z.C. Liu, W. Liu, Numerical investigation of shell side performance of a double shell side rod baffle heat exchanger, *Int. J. Heat Mass Tran.* 108 (2017) 2029–2039.
[19] X.T. Wang, Y.M. Liang, Y. Sun, Z.C. Liu, W. Liu, Experimental and numerical investigation on shell-side performance of a double shell-pass rod baffle heat exchanger, *Int. J. Heat Mass Tran.* 132 (2019) 631–642.
[20] Y.Y. Yuan, J.M. Cao, Z. Zhang, Z.Y. Xiao, X.S. Wang, Experimental and numerical simulation study of a novel double shell-passes multi-layer helically coiled tubes heat exchanger, *Int. J. Heat Mass Tran.* 227 (2024) 125497.
[21] S.F. Song, Numerical studies on performance of double shell-pass heat exchangers with sleeve tubes and continuous helical baffles, *Proc. CSEE* 33 (14) (2013) 82–87.
[22] X.H. Xu, J.H. Guo, Y.G. Lei, F. Wang, Heat transfer and flow resistance performance of a double shell-pass shell-and-tube heat exchanger, *J. Eng. Therm. Energy Power* 33 (12) (2018) 20–25.
[23] S. Ji, W.J. Du, P. Wang, L. Cheng, Numerical investigation on double shell-pass shell-and-tube heat exchanger with continuous helical baffles, *J. Thermodyn.* 2011 (1) (2011) 839468.
[24] J.F. Yang, M. Zeng, Q.W. Wang, Numerical investigation on shell-side performances of combined parallel and serial two shell-pass shell-and-tube heat exchangers with continuous helical baffles, *Appl. Energy* 139 (2015) 163–174.
[25] D. Raut, S. Londhe, V.R. Kalamkar, Performance investigation of latent heat energy storage in series and parallel arrangement: a numerical study, *J. Energy Storage* 55 (2022) 105678.
[26] A. Miyara Jalaluddin, R. Tarakka, Ilahi Ramadhani, Experimental performance analysis of shallow spiral-tube ground heat exchangers in series and parallel configurations, *E3S Web Conf.* 130 (2019) 01017.
[27] S.E. Sofyan, T.M.I. Riayatsyah, E. Hu, A. Tamlicha, T.M. Reza Pahlefi, H.B. Aditiya, Computational fluid dynamic simulation of earth air heat exchanger: a thermal performance comparison between series and parallel arrangements, *Results Eng.* 24 (2024) 102932.
[28] J.C. Lemos, A.L.H. Costa, M.J. Bagajewicz, Set trimming procedure for the design optimization of shell and tube heat exchangers, *Ind. Eng. Chem. Res.* 59 (31) (2020) 14048–14054.
[29] S.K. Bhatti, C.M. Krishna, C. Vundru, M.L. Neelapu, I.N. Niranjan Kumar, Estimating number of shells and determining the log mean temperature difference correction factor of shell and tube heat exchangers, *Adv. Comput. Meth. Heat Transf. IX* 1 (2006) 323–335.
[30] J.A.W. Gut, J.M. Pinto, Optimal configuration design for plate heat exchangers, *Int. J. Heat Mass Tran.* 47 (22) (2004) 4833–4848.
[31] A.L.H. Costa, M.J. Bagajewicz, 110th anniversary: on the departure from heuristics and simplified models toward globally optimal design of process equipment, *Ind. Eng. Chem. Res.* 58 (40) (2019) 18684–18702.
[32] Z.K. Yang, Y.J. Ma, N. Zhang, R. Smith, Design optimization of shell and tube heat exchangers sizing with heat transfer enhancement, *Comput. Chem. Eng.* 137 (2020) 106821.
[33] M. Pan, S. Jamaliniya, R. Smith, I. Bulatov, M. Gough, T. Higley, P. Droegemueller, New insights to implement heat transfer intensification for shell and tube heat exchangers, *Energy* 57 (2013) 208–221.

Appendix

Table A1
Design solutions for Min A

Example	1		2		3		4	
Heat exchanger type	Single	Double	Single	Double	Single	Double	Single	Double
Outer tube diameter, d_{te}/m	0.019	0.032	0.019	0.032	0.025	0.032	0.019	0.019
Tube length, L/m	6.098	6.098	6.098	6.098	2.439	3.049	3.659	4.877
Tube pitch ratio, r_p	1.25	1.25	1.25	1.25	1.33	1.33	1.25	1.50
Tube layout, l_{ay}	Square	Triangular	Triangular	Triangular	Square	Square	Triangular	Triangular
Shell diameter, D_s/m	1.219	1.524	0.787	1.067	0.787	0.787	0.838	0.838
Number of baffles, N_b	10	10	10	14	5	6	4	10
Number of tube passes, N_{pt}	2	4	4	4	4	4	6	4

Table A2
Optimisation results for Min A

Example	1		2		3		4	
Area/m^2	678.5	684.2	326.5	335.3	71.5	69.9	209.0	193.3
Temperature correction coefficient, F	0.931	0.984	0.929	0.984	0.913	0.980	0.813	0.961
Total number of tubes, N_{tt}	1864	1116	897	547	373	228	957	664
Baffle spacing, l_{bc}/m	0.55	1.02	0.55	0.76	0.41	0.76	0.73	0.82
Tube pitch, l_{tp}/m	0.024	0.040	0.024	0.040	0.033	0.043	0.024	0.029
Shell-side flow velocity, v_s/m·s^{-1}	1.04	0.90	0.73	0.78	2.24	2.39	1.01	1.09
Tube-side flow velocity, v_t/m·s^{-1}	1.27	1.27	1.51	1.48	1.31	1.22	1.46	1.40
Shell-side heat transfer coefficient, h_s/W·m^{-2}·K^{-1}	1053.39	891.35	1001.53	823.34	2684.62	2489.05	5221.46	3943.95
Tube-side heat transfer coefficient, h_t/W·m^{-2}·K^{-1}	5934.83	5258.83	6778.30	5918.62	10961.9	9825.24	12776.2	12374.4
Overall heat transfer coefficient, U/W·m^{-2}·K^{-1}	533.75	496.34	562.96	507.03	1373.27	1313.08	1839.90	1643.07
Shell-side pressure drop, ΔP_s/Pa	95659	73263	47638	53853	51836	50692	49885	53798
Tube-side pressure drop, ΔP_t/Pa	20409	22444	27602	29540	11914	9920	37321	28894

Table A3
Design solutions for Min TAC

Example	1		2		3		4	
Heat exchanger type	Single	Double	Single	Double	Single	Double	Single	Double
Outer tube diameter, d_{te}/m	0.019	0.025	0.019	0.032	0.038	0.038	0.025	0.025
Tube length, L/m	6.098	4.877	6.098	6.098	3.659	3.659	4.877	4.877
Tube pitch ratio, r_p	1.25	1.25	1.25	1.25	1.25	1.50	1.25	1.33
Tube layout, l_{ay}	Triangular	Triangular	Triangular	Triangular	Square	Square	Square	Square
Shell diameter, D_s/m	1.219	1.524	0.787	1.067	0.940	1.143	0.991	0.991
Number of baffles, N_b	5	6	9	14	3	6	7	8
Number of tube passes, N_{pt}	1	4	1	4	4	4	4	4

Table A4
Optimisation results for Min TAC

Example	1		2		3		4	
Cost TAC/USD	6261	17173	31229	3343	2303	2258	8400	7407
Area/m^2	805.1	700.2	335.60	460.5	114.0	117.1	256.3	226.4
Total number of tubes, N_t	2212	1828	922	791	261	268	669	591
Baffle spacing, l_{bc}/m	1.02	1.22	0.61	0.81	0.92	0.92	0.61	0.98
Tube pitch, l_{tp}/m	0.024	0.031	0.024	0.047	0.047	0.057	0.031	0.033
Shell-side flow velocity, v_s/m·s^{-1}	0.57	0.75	0.66	0.51	1.03	1.02	1.02	1.03
Tube-side flow velocity, v_t/m·s^{-1}	0.54	1.36	0.73	0.70	0.73	0.71	0.73	0.82
Shell-side pressure drop, ΔP_s/Pa	25344	44947	36438	21457	8181	8005	48052	41426
Tube-side pressure drop, ΔP_t/Pa	2062	27603	3570	5278	3617	3438	6296	7949

Table A5
Design solutions for automatic series-parallel connection

Heat exchanger arrangement	Series-Parallel arrangement	Series-Parallel arrangement
Heat exchanger type	Single	Double
Heat exchanger arrangement	Parallel	Parallel
Number of heat exchangers	8	16
Outer tube diameter, d_{te}/m	0.019	0.025
Tube length, L/m	6.098	6.098
Tube pitch ratio, r_p	1.33	1.50
Tube layout, l_{ay}	Triangular	Triangular
Shell diameter, D_s/m	1.524	1.372
Number of baffles, N_b	4	4
Number of tube passes, N_{pt}	2	4

Table A6
Optimisation results for automatic series-parallel connection

Heat exchanger arrangement	Series-Parallel arrangement	Series-Parallel arrangement
Heat exchanger type	Single	Double
Cost (Total), TAC/USD	601184	205040
Cost, TAC/USD	75148	12815
Area/m^2	1081.8	492.8
Total number of tubes, N_{tt}	2972	1029
Baffle spacing, l_{bc}/m	1.22	1.22
Tube pitch, l_{tp}/m	0.025	0.038
Shell-side flow velocity, v_s/m·s^{-1}	1.25	1.04
Tube-side flow velocity, v_t/m·s^{-1}	0.73	1.11
Shell-side pressure drop, ΔP_s/Pa	97673	26538
Tube-side pressure drop, ΔP_t/Pa	5197	16544